

Electronic Supplementary Information

Enhancement of photovoltaic properties of Ag_2BiI_5 by doping of Cu

Jin Woo Park,^{a,1} Yeongsu Lim,^{a,1} Kyung-Yeon Doh,^b Min Tai Jung,^a Young In Jeon,^a In Seok Yang,^a Hyeon-seo Choi,^a Jeongho Kim,^{a,*} Donghwa Lee^{b,*} and Wan In Lee^{a,*}

^a*Department of Chemistry and Chemical Engineering, Inha University, Incheon 22212, Korea*

^b*Department of Materials Science and Engineering and Division of Advanced Materials Science, Pohang University of Science and Technology (POSTECH), Pohang, Korea*

*Corresponding authors

W. I. Lee (E-mail: wanin@inha.ac.kr); J. Kim (E-mail: jkim5@inha.ac.kr); D. Lee (E-mail: donghwa96@postech.ac.kr)

¹ These authors contributed equally.

Table S1. Fitting parameters for each solar cell device with single exponential function,

$$I(t) = A e^{-t/\tau} + B.$$

Light absorber	τ (ns)	A	B
SBI	489	2.739	0.729
Cu2.5:SBI	413	0.904	0.434
Cu5:SBI	349	0.749	0.504
Cu10:SBI	256	0.732	0.203

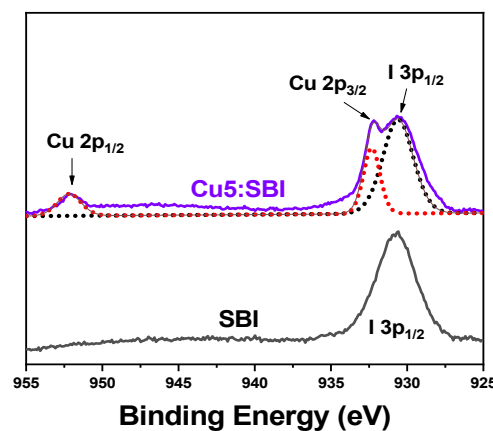
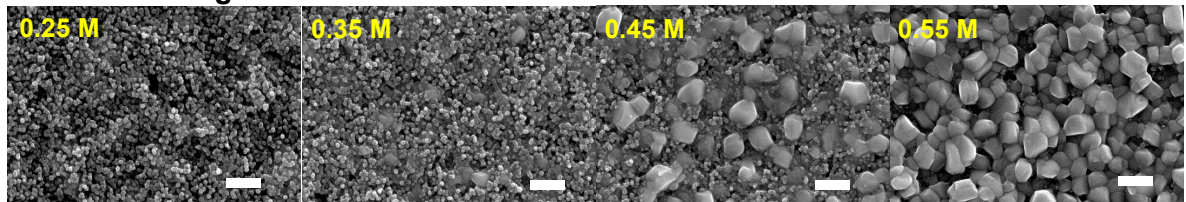


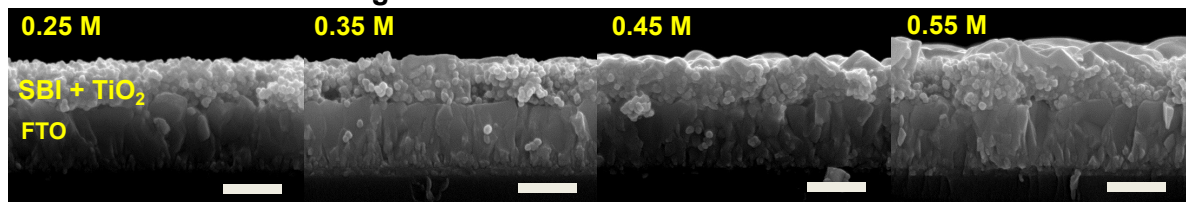
Fig. S1 XPS spectra of Cu 2p for the as-prepared SBI and Cu5:SBI powders.

(a)

Plan-view images

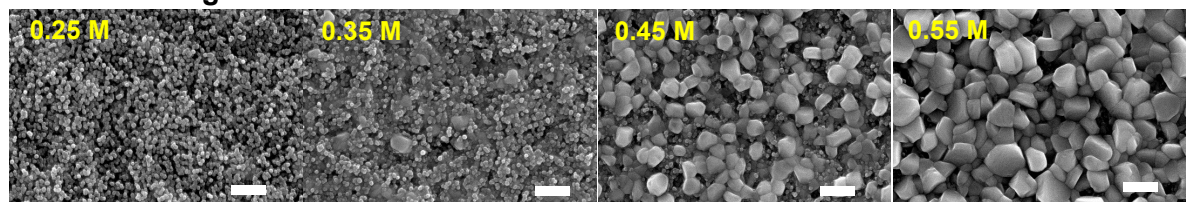


Cross-sectional view images



(b)

Plan-view images



Cross-sectional view images

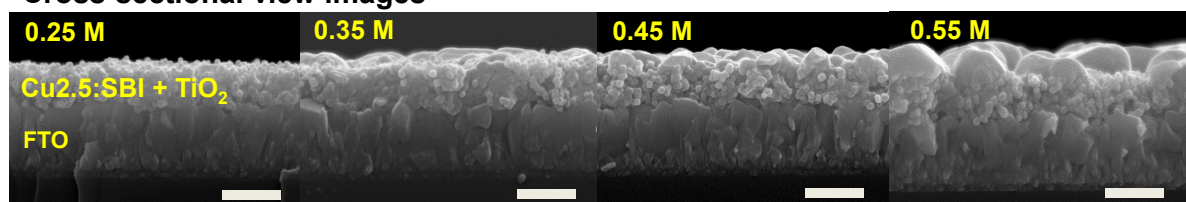


Fig. S2 SEM images of bare SBI (a) and Cu2.5:SBI (b) films coated on the mesoporous TiO₂ layer using the coating solutions of various concentrations. All scale bars indicate 500 nm.

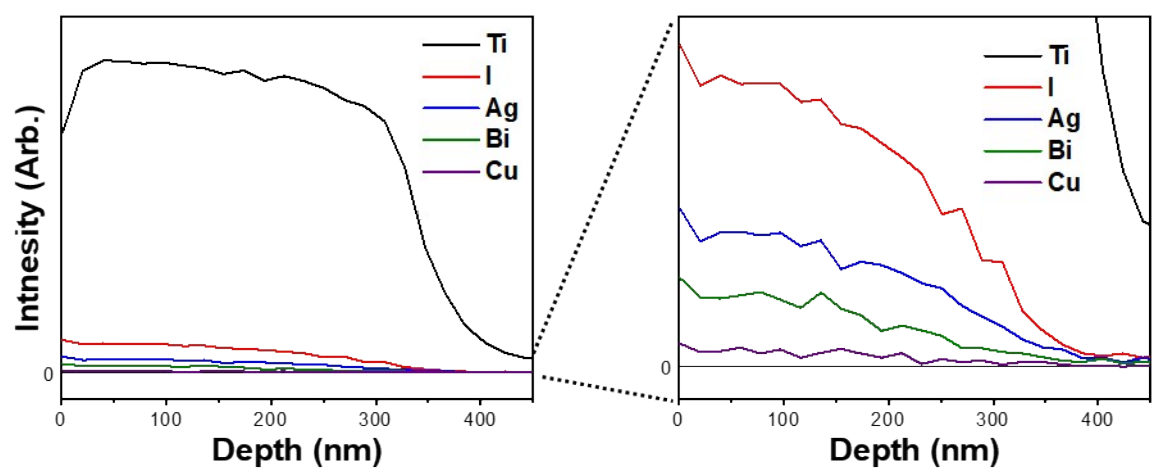


Fig. S3 Depth profile for the atomic composition for a Cu_{2.5}:SBI film coated on a mesoporous TiO₂ layer. Secondary ion mass spectrometer (SIMS, AMETEK, IMS 4FE7) was applied for the data acquisition.

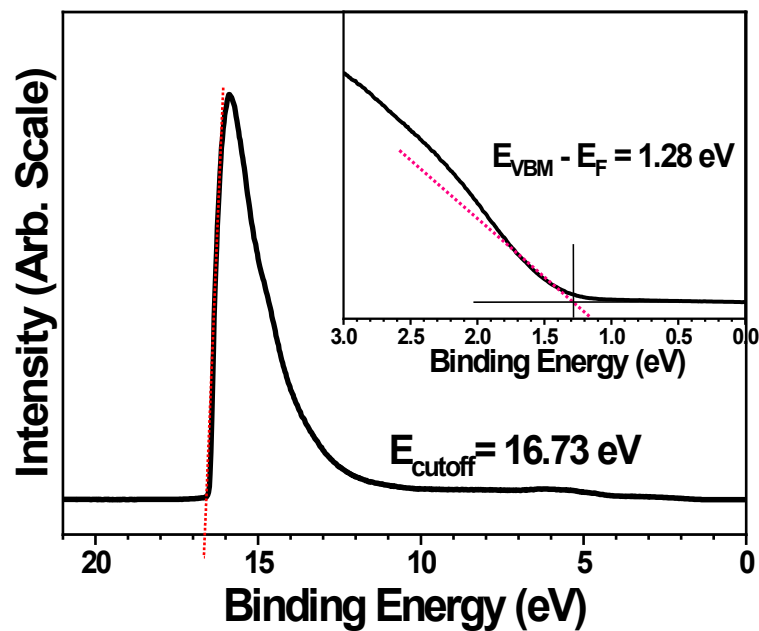
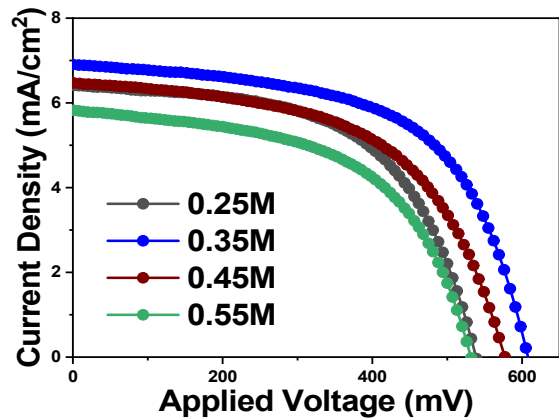
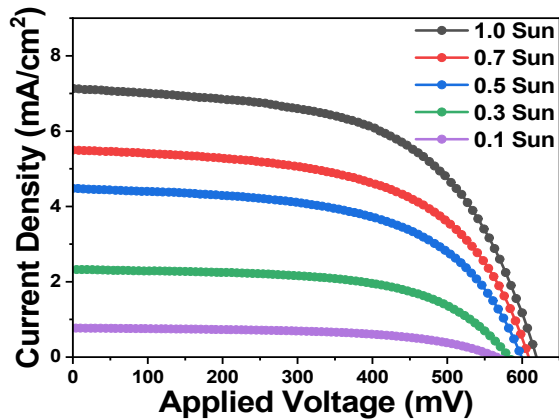


Fig. S4 UPS spectrum for the high binding-energy region of SBI film coated on a mesoporous TiO₂ layer while its low-binding-energy region is shown in the inset.



Concentration for Cu2.5:SBI coating	V _{OC} (mV)	J _{SC} (mA/cm ²)	FF (%)	PCE (%)
0.25M	538	6.41	57.64	1.99
0.35M	608	6.91	58.61	2.46
0.45M	577	6.47	55.18	2.06
0.55M	532	5.83	54.90	1.70

Fig. S5 J-V curves and PV parameters of various SC-Cu2.5:SBI devices depending on the concentration of coating solution in preparing Cu2.5:SBI films.



Cu2.5:SBI	V_{oc} (mV)	J_{sc} (mA/cm ²)	FF (%)	PCE (%)
1.0 sun	619	7.13	57.25	2.53
0.7 sun	609	5.50	56.81	2.72
0.5 sun	599	4.48	56.42	3.03
0.3 sun	582	2.32	58.18	2.62
0.1 sun	566	0.77	56.22	2.45

Fig. S6 $J-V$ curves of the SC-Cu2.5:SBI measured under various light intensities.

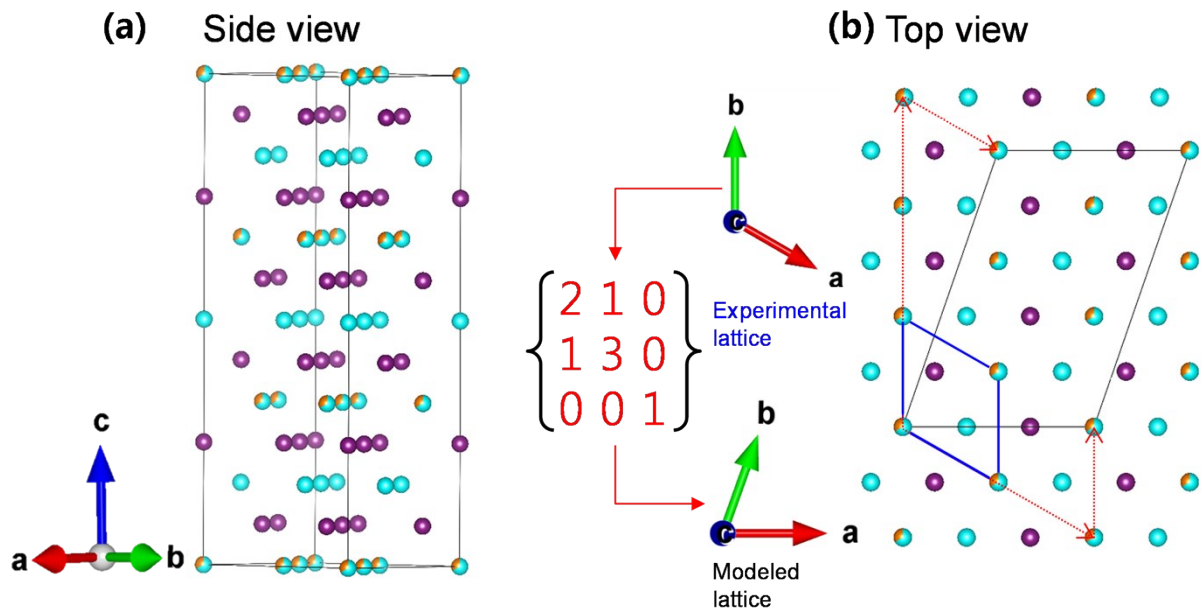


Fig. S7 (a) The modeled $\text{Ag}_{12}\text{Bi}_6\text{I}_{30}$ structure of SBI (Ag_2BiI_5). (b) The $\text{Ag}_{12/5}\text{Bi}_{6/5}\text{I}_6$ cell (blue) is transformed to $\text{Ag}_{12}\text{Bi}_6\text{I}_{30}$ supercell (black) by multiplying matrix $[[2,1,0],[1,3,0],[0,0,1]]$ (red arrow).

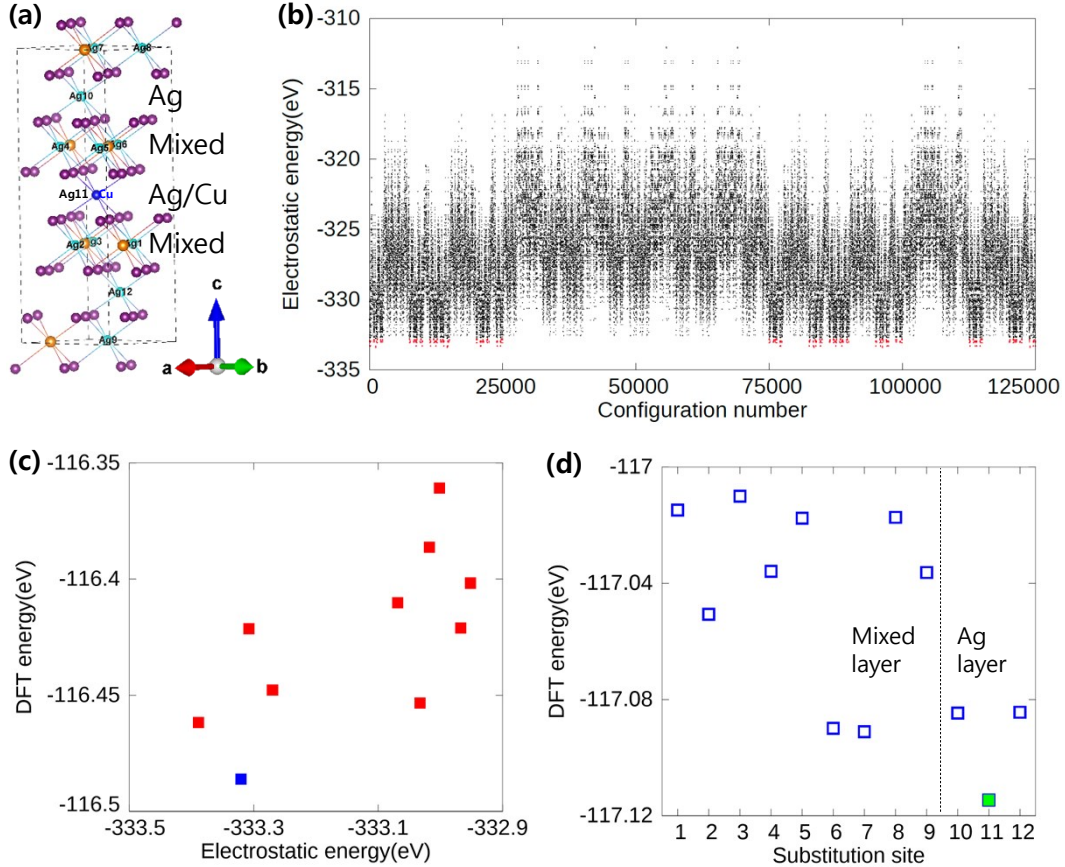


Fig. S8 (a) The modeled structure of Cu-doped SBI. (b) The electrostatic energy based on the formal charge of I(-1), Ag(+1), and Bi(+3) for all possible configurations of partially occupied $\text{Ag}_{12}\text{Bi}_6\text{I}_{30}$ (SBI). The 10 most energetically favorable configurations are selected based on the electrostatic energy. (c) Comparison on energetics obtained from DFT and electrostatic calculations for 10 selected SBI configurations. The lowest DFT energy configuration is shown by the blue filled square. (d) The comparison on the DFT energies of 12 different Cu substitutions in the Cu-doped SBI model. The DFT energy for the lowest energy configuration is indicated by the green filled square.

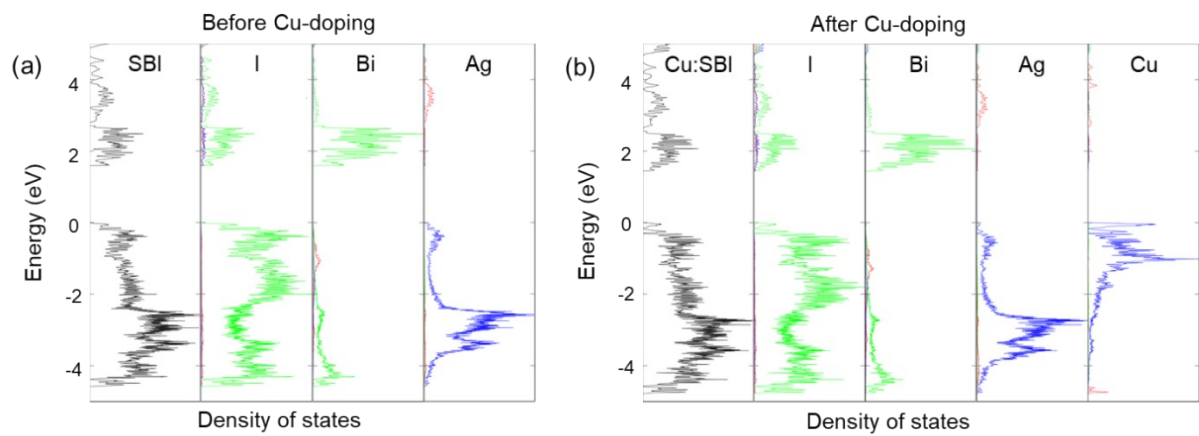


Fig. S9 Accumulated orbital decomposed partial density of states of I p-orbital, Bi p-orbital, Ag d-orbital, Cu d-orbital of SBI (a) and Cu:SBI (b).